Marine Environmental Research 202 (2024) 106717

Contents lists available at ScienceDirect

Marine Environmental Research

journal homepage: www.elsevier.com/locate/marenvrev

Transcriptomic analysis of the response mechanisms of black rockfish (*Sebastes schlegelii*) under noise stress from offshore wind farms

Yining Wang [a], Kuangmin Gong [b], Jun Xie [b], Wei Wang [b], Jianhao Zheng [b], Liuyi Huang [a,*]

[a] College of Fisheries, Ocean University of China, Qingdao, 266000, China
[b] Zhangpu Strait Power Generation Co. Ltd, Zhangzhou, 363000, China

ARTICLE INFO

Keywords:
Offshore wind farm
Noise
Sebastes schlegelii
Transcriptomic
KEGG analysis
Low-frequency

ABSTRACT

During the operational phase of offshore wind farms, the generation of low-frequency underwater noise has received widespread attention due to its potential adverse impact on fish health. This study conducted a field survey of underwater noise at offshore wind farms located in Shandong province, China. Subsequently, a small-scale experiment was conducted to study the stress on black rockfish (*Sebastes schlegelii*). The fish were exposed to noise with dominant frequency of 80 Hz, 125 Hz and 250 Hz. These frequencies are same with the frequencies from wind power noise (wpn) at the actual site. After a 40-day experimental period, transcriptome sequencing was conducted on brain, liver, and kidney tissues of black rockfish to elucidate the underlying molecular mechanisms involved in the response to noise stress originating from offshore wind farms. The results revealed that the 125 Hz group exhibited the highest number of differentially expressed genes (DEGs) between the noise-exposed and control check group (CK group), with a total of 797 in the brain, 1076 in the liver, and 2468 in the kidney. Gene Ontology (GO) analysis showed that DEGs were significantly enriched in entries related to cellular processes, membrane components, binding, and metabolism. Kyoto Encyclopedia of Genes and Genomes (KEGG) analysis showed that DEGs were enriched mainly in metabolism, immunity, apoptosis, signal transduction, and diseases. The findings indicate that prolonged exposure to underwater noise from offshore wind farms may induce metabolic imbalance, immune dysfunction, and an increased risk of myocardial diseases in black rockfish.

1. Introduction

Offshore wind power, as a type of clean and green energy, emits no pollutants or carbon dioxide during its development process. It is beneficial for energy balance and holds significant environmental value (Ali et al., 2021). In Europe, the first commercial offshore wind farm began operating in Denmark, and subsequently, offshore wind markets in countries like the United Kingdom, Germany, and the Netherlands experienced rapid growth. Following this, the scale of offshore wind farms and floating offshore wind power expanded rapidly in non-European countries such as the United States and Japan (Higgins and Foley, 2014; Soares-Ramos et al., 2020; Li, 2022). To achieve its goal of becoming carbon neutral by 2060, China is actively developing wind power to reduce its dependence on fossil fuels (Chen and Lin, 2022). The demand for electricity is substantial, particularly in China's coastal regions characterized by high population density and economic development. The unique geographical characteristics of these coastal areas offers favorable conditions for offshore wind power (Chen et al., 2022). The installed offshore wind power capacity in China has increased from 4.53 GW in 2014 to 30.51 GW in 2022 (Zhongshang Industrial Research Institute).

However, the operation of offshore wind turbines generates a variety of low-frequency noise in the underwater environment. Kulkarni and Edwards (2022) indicated that noise from offshore wind farms can be potential hazards to marine organisms and fisheries. The majority of fish possess auxiliary organs such as swim bladders and lateral lines that enable them to receive sounds, making them particularly sensitive to underwater noise pollution. The operational noise generated by offshore wind farms falls within the low-frequency range (<700 Hz), which coincides with the frequency spectrum of fish communication, mating, spawning, and spatial movement (Cresci et al., 2023). This overlap may potentially have negative impacts on the health of fish. Consequently, research on the impact of wind power noise (wpn) on fish behavior and physiology has attracted widespread attention (Winter et al., 2010; Popper and Arthur, 2022).

At present, how the wpn affects fish physiology is not yet clear. The

* Corresponding author.
E-mail address: huangly@ouc.edu.cn (L. Huang).

https://doi.org/10.1016/j.marenvres.2024.106717
Received 10 May 2024; Received in revised form 22 July 2024; Accepted 28 August 2024
Available online 30 August 2024

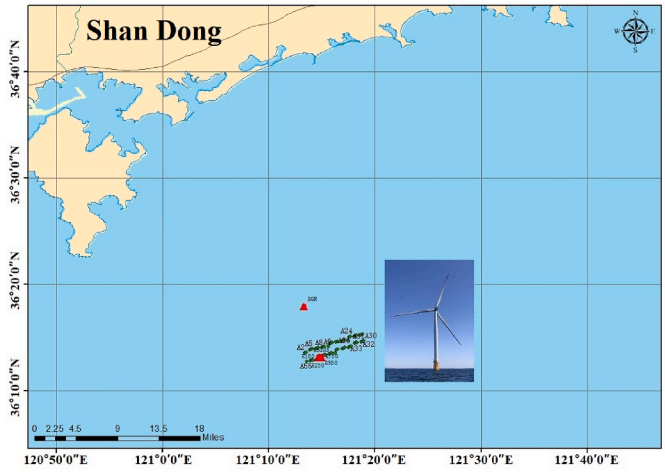

Fig. 1. The location of offshore wind farm of Shandong. The green mark indicates wind turbine position, and the red mark indicates measurement point position. 'BGN' stands for the location where background noise was collected.

effects of noise on fish have focused on hearing loss and stress response (Smith et al., 2004; Sierra-Flores et al., 2015; Smith and Arthur, 2023). Mann et al. (2007) conducted experiments with nine spine sticklebacks *(Pungitius*) and measured their hearing sensitivity. The auditory system was most sensitive at 100–200 Hz (approximately 90–100 dB re 1 μPa) and decreased at 400 Hz and above to >113 dB re 1 μPa. Buscaino et al. (2010) reported significant changes in haematological responses (increase in lactate and haematocrit levels and decrease of glucose) in European sea bass (*D. labrax*) and gilthead seabream (*S. aurata*) in response to noise. The authors also reported that when fish were exposed to noise, a linear correlation was found between blood parameters and motility (Buscaino et al., 2010). Chang et al. (2018) reported that the long-term (2 weeks) physiological effects of simulated wind farms noise (138 dB re1 μPa/125.4 Hz; near the turbine) on black porgies (*Acanthopagrus schlegelii*) caused a significant increase in cortisol and ROS in these fish.

Transcriptome profiling has been widely used in fish for effective identification and expression analysis of candidate genes involved in growth, reproduction, development, immunity, disease, stress and toxicology (Chandhini, 2019). The study conducted by Schuck et al. (2011) shown that exposure to noise can induce damage to the sensory hair cells in the inner ears of zebrafish (*Danio rerio*). Using gene chip technology, Andrews et al. (2014) conducted transcriptomic analysis on 79 specific transcripts in Atlantic salmon (*Salmo salar*) before and after exposure to noise. They observed an upregulation of transcripts associated with neural cell damage, particularly those encoding nicotinamide riboside kinase 2, indicating potential inner ear neuron damage in Atlantic salmon due to noise exposure. The impact of noise on the auditory system of channel catfish (*Ictalurus punctatus*) was investigated by Yang et al. (2018) through transcriptome analysis of the swim bladder. Butler and Maruska (2021) exposed gravid female African cichlids (*Astatotilapia burtoni*) to excessive ocean ambient noise at 140 dB for a duration of 3 h, resulting in alterations in the brain transcriptome of the hatching fry and increased mortality rates. The study conducted by Zhang X et al. (2022) revealed that exposure to ship noise at a sound intensity of 120 dB resulted in the manifestation of neurological dysfunction and impaired motor ability in yellow croaker (*Larimichthys polyactis*). Mai (2018) demonstrated that exposure to ship noise at 132 dB led to the upregulation of transcripts associated with key metabolic pathways, including the citric acid cycle, pentose phosphate pathway, and oxidative phosphorylation, in the liver of *Sebastiscus marmoratus*. Zhang Y et al. (2022) conducted a comprehensive multi-omics investigation on hybrid sturgeon (*Acipenser baerii* ♀ × *Acipenser schrenckii*♂) subjected to ship-induced noise for a duration of 12 h, elucidating an upregulation of apoptosis and enhanced cellular motility in the liver, alongside suppression of protein synthesis and metabolism-associated pathways. Furthermore, the impact of noise extends to marine invertebrates. The study conducted by Cheng et al. (2024) revealed that the low-frequency noise emitted by offshore wind farms exerts a suppressive influence on apoptosis in the intestinal cells of sea cucumber (*Apostichopus japonicus*), resulting in diminished cell motility and disruption of lipid metabolism processes as well as membrane synthesis. Tu et al. (2021) indicated that low-frequency noise significantly impacts the transcriptome of the central nervous system in *Onchidium reevesii*, a stone centipede species. This influence is observed in various energy metabolism pathways, including cytokine-receptor interactions, FoxO signaling, apoptosis and immune-related pathways, glycolysis, TCA cycle, glycerophospholipid metabolism. Additionally, it affects neural pathways such as GABAergic synapses, synaptic vesicle cycling, amyotrophic lateral sclerosis (ALS), and other relevant networks. Hall et al. (2023) observed significant differential expression of liver and pancreas transcripts associated with stress and immune responses in snow crab (*Chionoecetes opilio*) following a prolonged exposure period of 22 weeks to seismic airgun noise.

Several studies suggest that around 100 species within the Sebastes genus may exhibit strong habitat fidelity (Matthews, 1990; Kendall, 1991; Love et al., 2022), potentially considering offshore wind turbines as their preferred habitat. This could result in long-term sublethal effects caused by the underwater noise generated during the operational phase of offshore wind farms (Cheng et al., 2024). *Sebastes schlegelii*, commonly referred to as the black rockfish, is a teleost fish belonging to the Sebastidae family within the Scorpaeniformes order and Sebastes genus. It predominantly inhabits waters adjacent to rocky reefs and is primarily distributed in the coast of Chinese Bohai Sea and Yellow Sea, Japan, and the Korean Peninsula. Being a pivotal marine economic species in Asia, it also holds significant importance in cage aquaculture in the area. The species exhibits a wide distribution across offshore wind farms established in Bohai Sea and Yellow Sea. This study focuses on juvenile *S. schlegelii*, utilizing offshore wind turbine dominant frequency noise measurements and on-site noise recordings to conduct controlled stress experiments in aquaculture farm tanks setting. Tissues of the brain, liver, and kidney were dissected for subsequent transcriptome sequencing analysis. The analysis of DEGs, GO analysis, and KEGG analysis aims to elucidate the underlying response mechanisms of juvenile *S. schlegelii* to noise stress originating from offshore wind farms. The results of this study can provide scientific insights for optimizing the design of offshore wind turbines, conducting environmental assessments of offshore wind farms, and facilitating rational layouts for 'wind-fish integration'.

2. Materials and methods

2.1. Recording of offshore wind farm noise sources

The underwater noise data were derived from recordings acquired by the authors in June 2022 at a specific geographical location (121°13′-121°19′ E, 36°12′-36°16′ N) of a 5.2 MW single-pile foundation wind turbine situated in Shandong, China (Fig. 1). The turbine was positioned 35 km offshore, with a water depth of 30 m and a wind speed of 2.1 ± 1.4 m/s. The underwater noise was recorded using a MARS 2.0 acoustic recorder, which was connected to an SPH32R piezoelectric hydrophone with a frequency response range of 1 Hz–30 kHz and a sensitivity of −182 dB. Sound pressure levels (SPLs) were measured at horizontal distances of 5 m, 50 m, 100 m, 250 m, 500 m, and 750 m from the turbine at water depths of 1 m, 3 m, 5 m, and 7 m. Each measurement lasted for 5 min, and the recorded data were processed using Matlab and Adobe Audition software. The dominant frequencies and their corresponding SPLs were determined through one-third octave band analysis. As shown in Fig. 2, the most frequent dominant frequencies were 80 Hz, 125 Hz, and 250 Hz, occurring 13 times, 10 times, and 7 times,

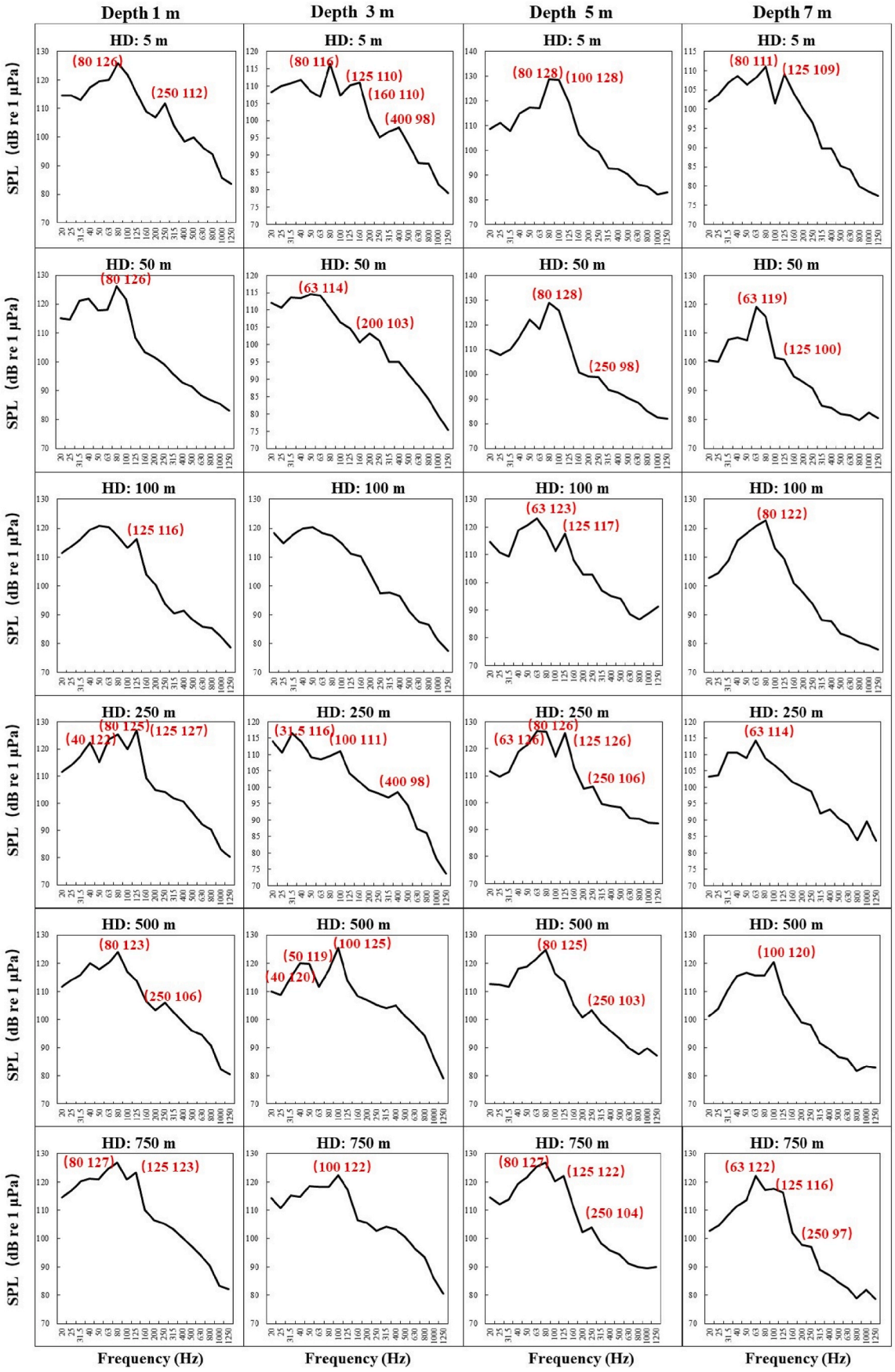

Fig. 2. Spectrum of horizontal distance noise at water depth of 1 m, 3 m, 5 m, 7 m
'HD' indicates horizontal distance. The numbers within the brackets indicates dominant frequency on the left and SPL on the right in the figure.

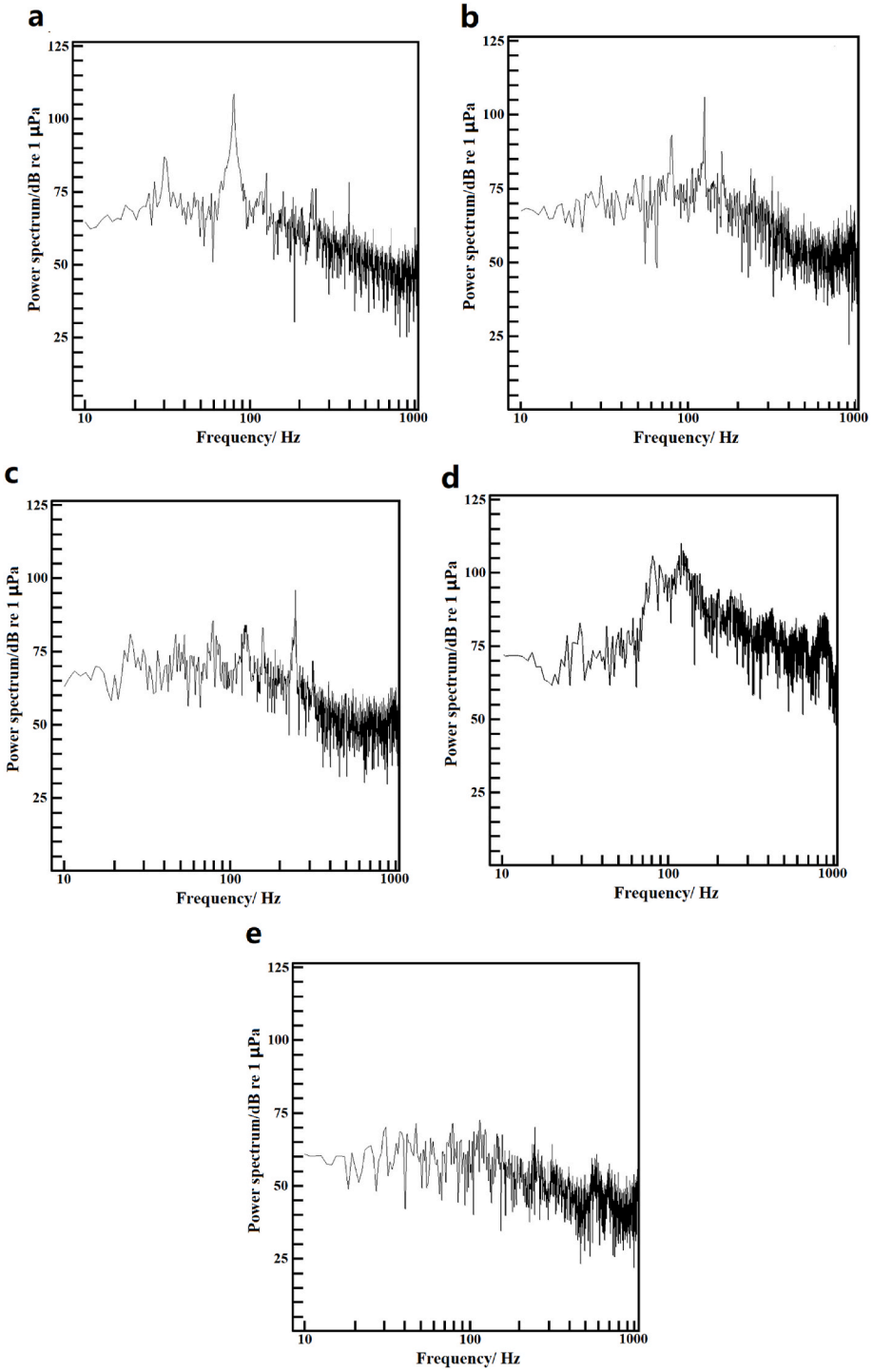

Fig. 3. Peak underwater sound spectrum of CK group and different noise groups.
a: 80 Hz group. b: 125 Hz group. c: 250 Hz group. d: wpn group. e: control group.

respectively. Based on the measured data, the calculated source levels for these three dominant frequencies were 151.9 dB, 147.47 dB, and 137.33 dB, respectively. The Kraken model was employed to compute the transmission loss at a horizontal distance of 5 m from the offshore wind farm (Jensen, 1982). Considering the habitat of the *S. schlegelii* predominantly in the mid-to-lower water column, transmission loss values were calculated for the mid-layer (15 m) and bottom layer (30 m) sea areas, yielding 43.01 dB, 44.58 dB, 48.32 dB, and 43.59 dB, 37.93 dB, 34.77 dB, respectively, for the respective layers. Averaging these values, the underwater sound intensity levels at the seabed were determined to be 108.60 dB, 106.22 dB, and 95.79 dB, respectively. The wpn was calculated by averaging the sound intensities from the nearest horizontal distance (5 m) across the four depth of water, resulting in a value of 107.42 dB.

2.2. Study species

Juvenile *S. schlegelii* were obtained from an aquaculture trial base in Yantai, Shandong Province, China. The fish had an average body length of 12.0 ± 0.72 cm and a weight of 30.8 ± 5.30 g, with a total quantity of

Table 1
Differentially expressed genes in the control group and noise exposure group.

Tissue	Regulate	Compare Group			
		CK vs 80 Hz	CK vs 125 Hz	CK vs 250 Hz	CK vs wpn
Brain	up	530	366	267	90
	down	205	431	257	60
Liver	up	341	461	206	179
	down	326	615	248	245
Kidney	up	189	964	102	288
	down	145	1504	128	471

400 individuals. Prior to the experiment, the fish were acclimatized to the experimental environment through a 2-week period of adaptation in a 4 m × 4 m × 0.7 m aquaculture pond. The water temperature was maintained at 9.0 ± 1.61 °C throughout the experimental period, while the levels of dissolved oxygen were consistently maintained at 6.1 ± 0.41 mg/L. The light-dark cycle was set at 13:11 h. During the acclimation period, fish were fed once daily at 13:00 with a feeding amount equivalent to 5% of their biomass. Moreover, the pond water was replenished daily at 7:00 a.m., with each refill comprising half of the total pond volume.

2.3. Experimental design

Several studies have demonstrated that the auditory sensitivity range of *S. schlegelii* extends from 80 to 300 Hz (Du-Ok, 2000; Wang et al., 2023). Based on the underwater noise measurements and the auditory sensitivity range of *S. schlegelii*, the present study established five experimental groups: 80 Hz, 125 Hz, 250 Hz, wpn group, and a control group with no noise exposure. The groups exhibited average sound intensities of 109.26 ± 2.76 dB, 106.40 ± 5.09 dB, 95.17 ± 4.58 dB, 107.42 ± 2.83 dB, and 66.48 ± 0.74 dB, respectively (Fig. 3). The noise

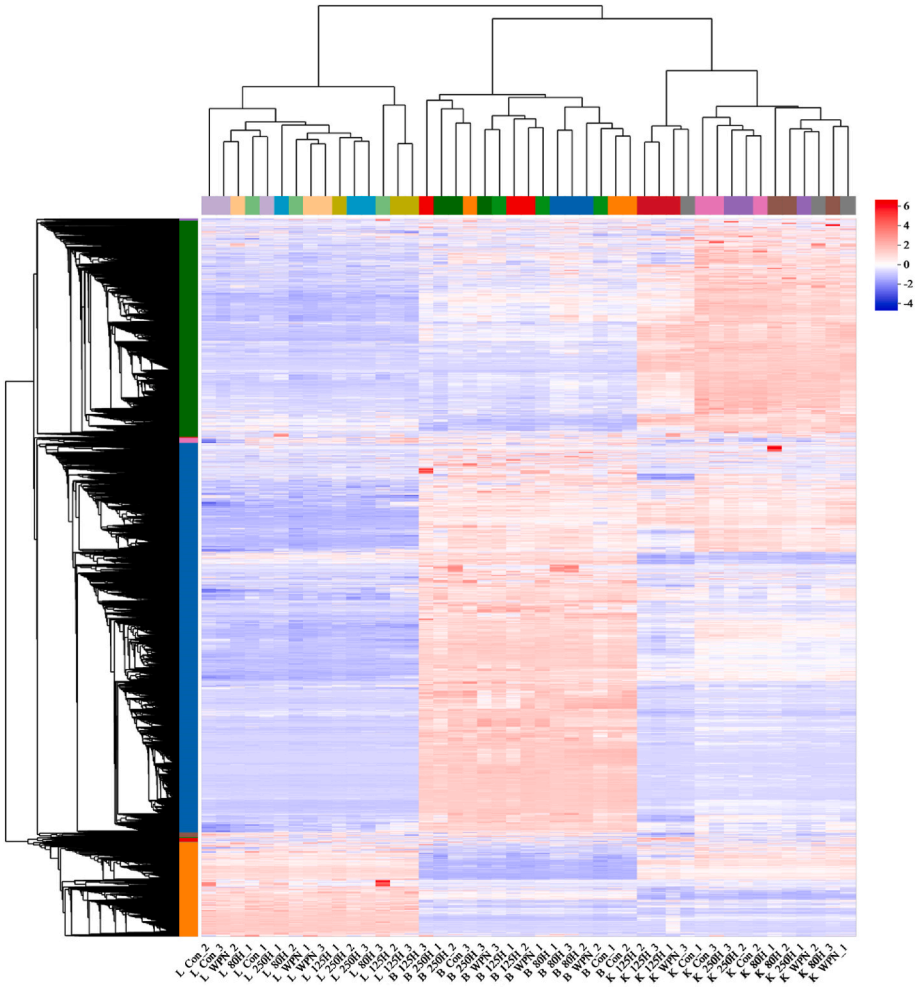

Fig. 4. Heatmap of DEGs between the control group and the noise exposure group. The horizontal axis is the sample name, and the vertical axis is the normalized value of the differential gene in TPM. Red color indicates up regulated genes and blue color indicates down regulated genes.
'B' indicates brain, 'L' indicates liver, 'K' indicates kidney.

Table 2
DEGs related to sound sensory perception in brain and kidney of *S. schlegelii.*

Tissue	Compare Group	Gene id	KO name	KO id	*P*-value	Regulate
Brain	80 Hz vs CK	*S.schlegelii*_GLEAN_10012965	*DCDC2*	K23405	0.039	down
Brain	125 Hz vs CK	*S.schlegelii*_GLEAN_10019761	*USH1C*	K21877	0.003	up
Kidney	80 Hz vs CK	*S.schlegelii*_GLEAN_10019761	*USH1C*	K21877	0.001	up
Kidney	125 Hz vs CK	*S.schlegelii*_GLEAN_10019458	*CLIC5*	K05025	7.15E-13	up

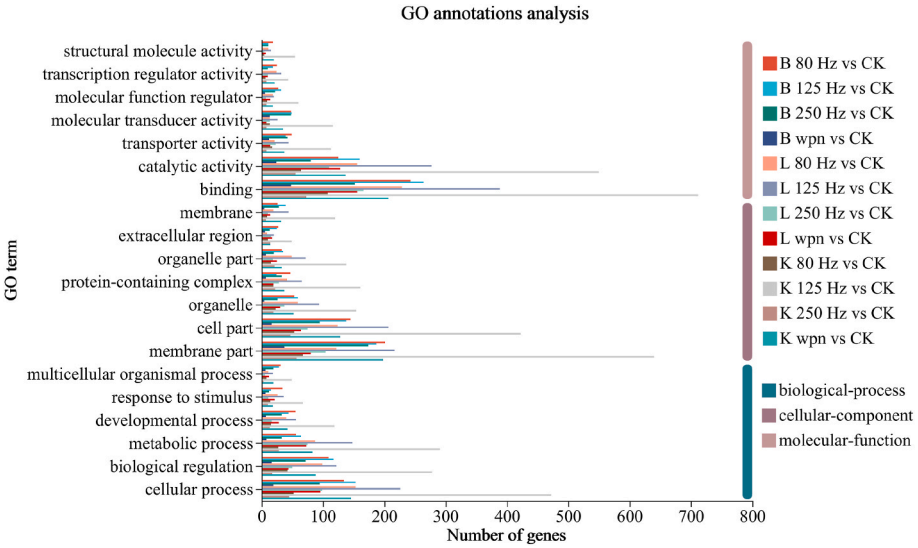

Fig. 5. The bar graph illustrates the statistics of GO classification for multiple gene sets, with different colors representing each gene set. 'B' indicates brain, 'L' indicates liver, 'K' indicates kidney.

stress experiment involved allocating twenty randomly selected experimental fish to each group, where the experimental groups were subjected to continuous sound exposure for 40 days (between December 2022 and January 2023), for 24 h each day (Popper and Hastings, 2009; Chen et al., 2014). A total of 45 fish were utilized in the experiment. Forty days after noise exposure, nine fish were randomly selected from each of the five groups by five assistants concurrently, with euthanasia and subsequent sampling conducted simultaneously. Euthanasia was performed using an overdose of tricaine methanesulfonate (MS-222), administered at a concentration that ensures rapid unconsciousness and minimal distress, followed by the cessation of gill movement. The concentration used was 300 mg/L of water, buffered with sodium bicarbonate to maintain a neutral pH, thus ensuring the well-being of the fish until loss of consciousness. Tissue samples from the brain, liver, and kidney were collected and immediately transferred into sterile tubes, then stored in liquid nitrogen for preservation before being transported to the laboratory for further analysis in a −80 °C ultra-low-temperature freezer. Upon completion of the experiments, all surviving fish were assessed by a qualified aquatic veterinarian to determine their health status and potential for release. Healthy fish, showing no signs of long-term harm from the study, were reintroduced to their native habitats in accordance with guidelines established by the local Department of Fisheries and Wildlife. This study was approved by the Animal Ethical Committee of Ocean University of China, Qingdao, China (No. OUC-AE-202206068).

2.4. Sample treatment

2.4.1. RNA extraction

Total RNA was extracted from the brain, liver and kidney tissues of *S. schlegelii* using TRIzol® Reagent according the manufacturer's instructions. Then RNA quality was determined by 5300 Bioanalyser (Agilent) and quantified using the ND-2000 (NanoDrop Technologies). Only high-quality RNA sample (OD260/280 = 1.8–2.2, OD260/230 ≥ 2.0, RIN≥6.5, 28S:18S ≥ 1.0, >1 μg) was used to construct sequencing library. The statistical power of this experimental design, calculated in RNASeqPower (An online implementation of RNASeqPower is available at https://rodrigo-arcoverde.shinyapps.io/rnaseq_power_calc/) is 0.83. There were 9 biological and technical replicates used to achieve the claimed statistical power.

2.4.2. Library preparation and sequencing

RNA purification, reverse transcription, library construction and sequencing were performed at Shanghai Majorbio Bio-pharm Biotechnology Co., Ltd. (Shanghai, China) according to the manufacturer's instructions (Illumina, San Diego, CA). The *S. schlegelii* RNA-seq transcriptome library was prepared following Illumina® Stranded mRNA Prep, ligation from Illumina (San Diego, CA) using 1 μg of total RNA. First, messenger RNA was isolated according to polyA selection method by oligo (dT) beads and then fragmented by fragmentation buffer. Secondly double-stranded cDNA was synthesized using a SuperScript double-stranded cDNA synthesis kit (Invitrogen, CA) with random hexamer primers (Illumina). Then the synthesized cDNA was subjected to end-repair, phosphorylation and 'A' base addition according to Illumina's library construction protocol. Libraries were size selected for cDNA target fragments of 300 bp on 2% Low Range Ultra Agarose followed by PCR amplified using Phusion DNA polymerase (NEB) for 15 PCR cycles. After quantified by Qubit 4.0, paired-end RNA-seq sequencing library was sequenced with the NovaSeq 6000 sequencer (2 × 150 bp read length). The raw sequence data reported in this paper have been deposited in the Sequence Read Archieve in National Center for Biotechnology Information (SRA: SRR28002100-SRR28002144) that are publicly accessible at http://www.ncbi.nlm.nih.gov/sra.

2.4.3. Quality control and read mapping

The raw paired end reads were trimmed and quality controlled by fastp with default parameters (Chen et al., 2018). Then clean reads were separately aligned to reference genome of *S. schlegelii* (GenBank accession no. CNA0000824) with orientation mode using HISAT2 software (Kim et al., 2015). The mapped reads of each sample were assembled by StringTie in a reference-based approach (Pertea et al., 2015).

2.4.4. Differential expression analysis and functional enrichment

The expression level of each transcript was calculated according to the transcripts per million reads (TPM) method. RSEM was used to quantify gene abundances (Li and Dewey, 2011). Essentially, differential expression analysis was performed using the DESeq2 (Love et al., 2014). DEGs with $|\log2FC| \geq 1$ and FDR < 0.05 were considered to be significantly different expressed genes. In addition, functional-enrichment analysis including GO and KEGG were performed to identify which DEGs were significantly enriched in GO terms and metabolic pathways at Bonferroni-corrected *P*-value < 0.05 compared with the whole-transcriptome background. GO functional enrichment and KEGG

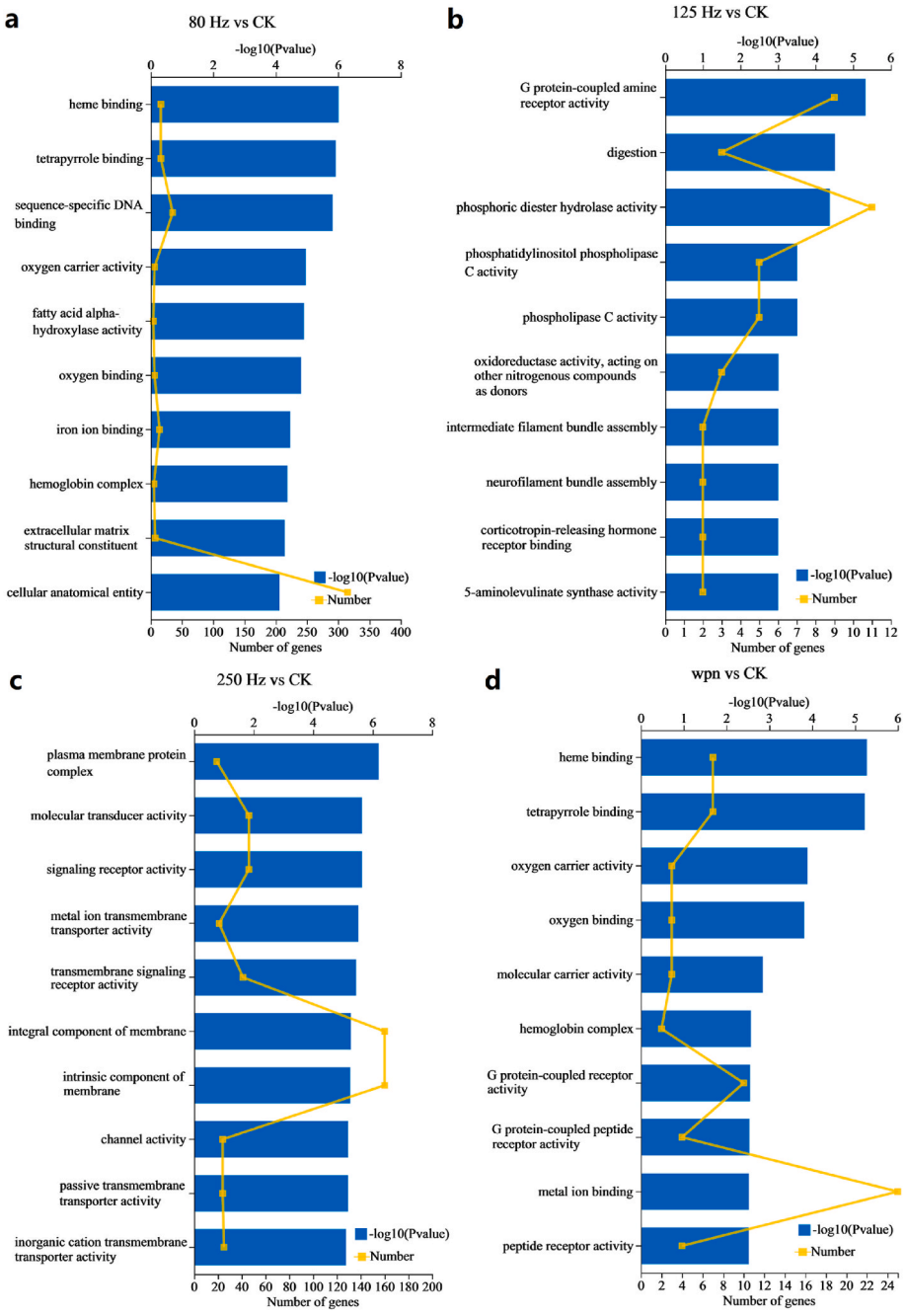

Fig. 6. The top 10 most significantly enriched GO terms from the differentially expressed genes of brain, with a *P*-value of <0.05. a: CK vs 80 Hz group. b: CK vs 125 Hz group. c: CK vs 250 Hz group. d: CK vs wpn group.

pathway analysis were carried out by Goatools and Python scripy, respectively.

2.4.5. Quantitative real-time PCR

Six differentially expressed genes were randomly selected from the brain, liver, and kidney tissues of *S. schlegelii* for qRT-PCR. The accuracy of reverse transcription was verified using the 2X Taq Plus Master Mix reagent kit for PCR validation, with the *β-actin* gene serving as the template. The relative mRNA expression levels of the target genes were calculated using the $2^{-\Delta\Delta Ct}$ method (Kenneth and Thomas, 2001). The PCR primers for the selected genes were designed using Primer Premier 5.0 software. The PCR procedure strictly followed the instructions provided by the ChamQ SYBR Color qPCR Master Mix (2X) reagent kit (P211/P212, Nanjing Novozymes Biological Technology Co., Ltd., Nanjing, China).

3. Results

A total of 338.59 Gb of clean data was obtained from the 45 samples in the experiment, with each sample yielding clean data of 6.01 Gb or more. The Q30 base percentage was consistently above 94.02%. A total of 28000 expressed genes were detected in the experiment, comprising 23375 known genes and 4625 novel genes. The expressed transcripts numbered 65998, with 22136 known transcripts and 43862 novel transcripts.

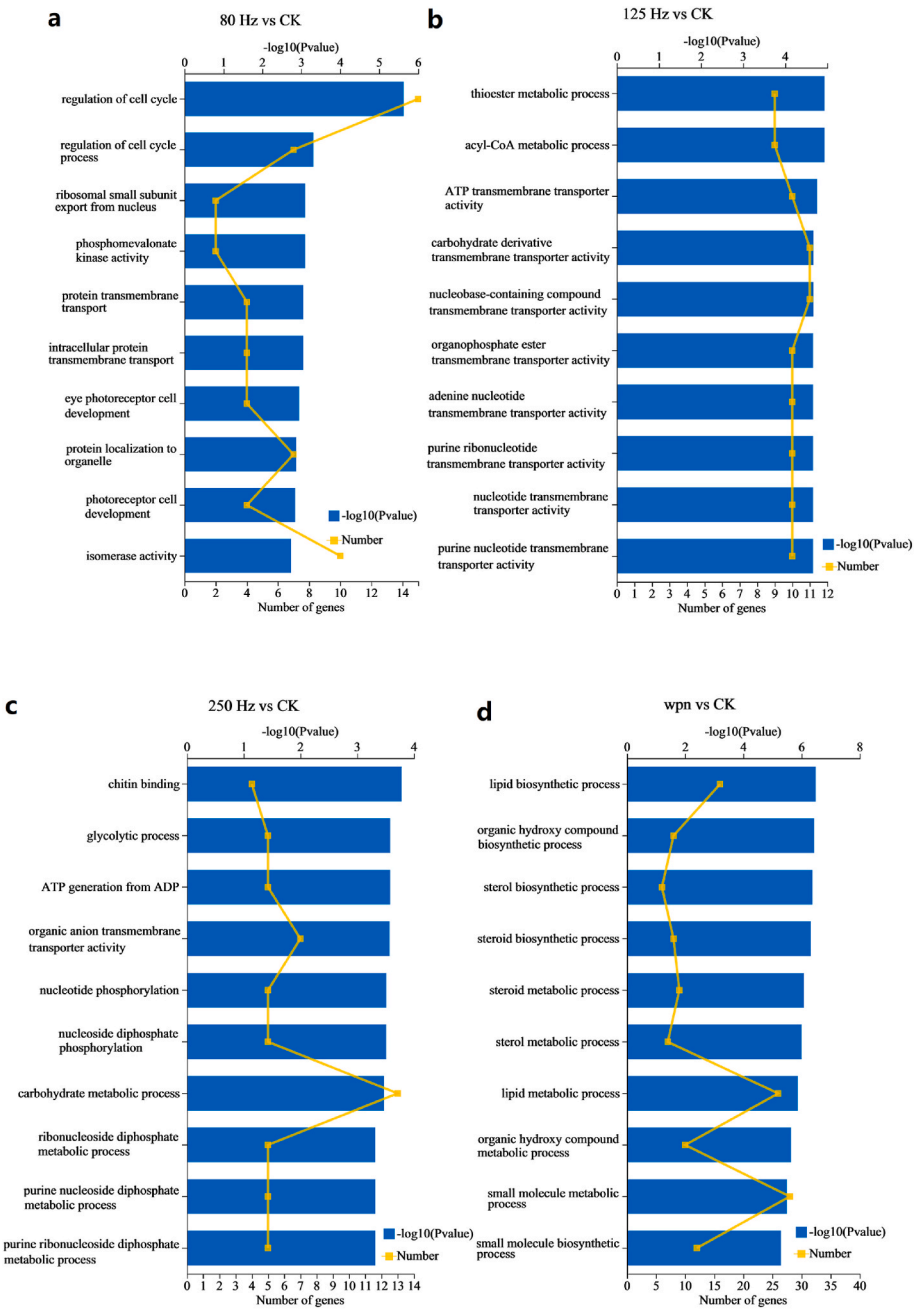

Fig. 7. The top 10 most significantly enriched GO terms from the differentially expressed genes of liver, with a *P*-value of <0.05. a: CK vs 80 Hz group. b: CK vs 125 Hz group. c: CK vs 250 Hz group. d: CK vs wpn group.

3.1. Analysis of DEGs

To elucidate the response mechanisms of *S. schlegelii* to different frequency noise stress, a comparative analysis was conducted on the significantly DEGs in the brain, liver, and kidney tissues between the CK group and the 80 Hz, 125 Hz, 250 Hz, and wpn groups (Table 1). In comparison to the CK group, the experimental groups of *S. schlegelii* exhibited varying degrees of differential gene expression across the three tissues. Among these, the 125 Hz group had the largest number of DEGs, followed by the 80 Hz group (except for kidney tissues), while the 250 Hz group and wpn group had relatively fewer DEGs. This indicates that the impact of the 125 Hz and 80 Hz frequencies on *S. schlegelii* is greater than that of the 250 Hz and wpn groups. In addition, the heatmap of the DEGs provided a visual illustration of the expression differences (Fig. 4), revealing a clear pattern that distinguished between the control and noise exposure groups.

The impact of noise on the health of fish may initially disrupt genes associated with their auditory perception. In this study, we identified DEGs related to sound sensory perception in the brain and kidney tissues of *S. schlegelii*, as presented in Table 2. In comparison to the CK group, three genes related to sound sensory perception were identified in the GO annotations of DEGs in the brain and kidney tissues of *S. schlegelii* across the experimental groups. Specifically, the *USH1C* gene was significantly downregulated in kidney tissues of the 80 Hz group and in brain tissues of the 125 Hz group. The *DCDC2* gene showed significant downregulation in brain tissues of the 80 Hz group, and the *CLIC5* gene exhibited significant upregulation in kidney tissues of the 125 Hz group.

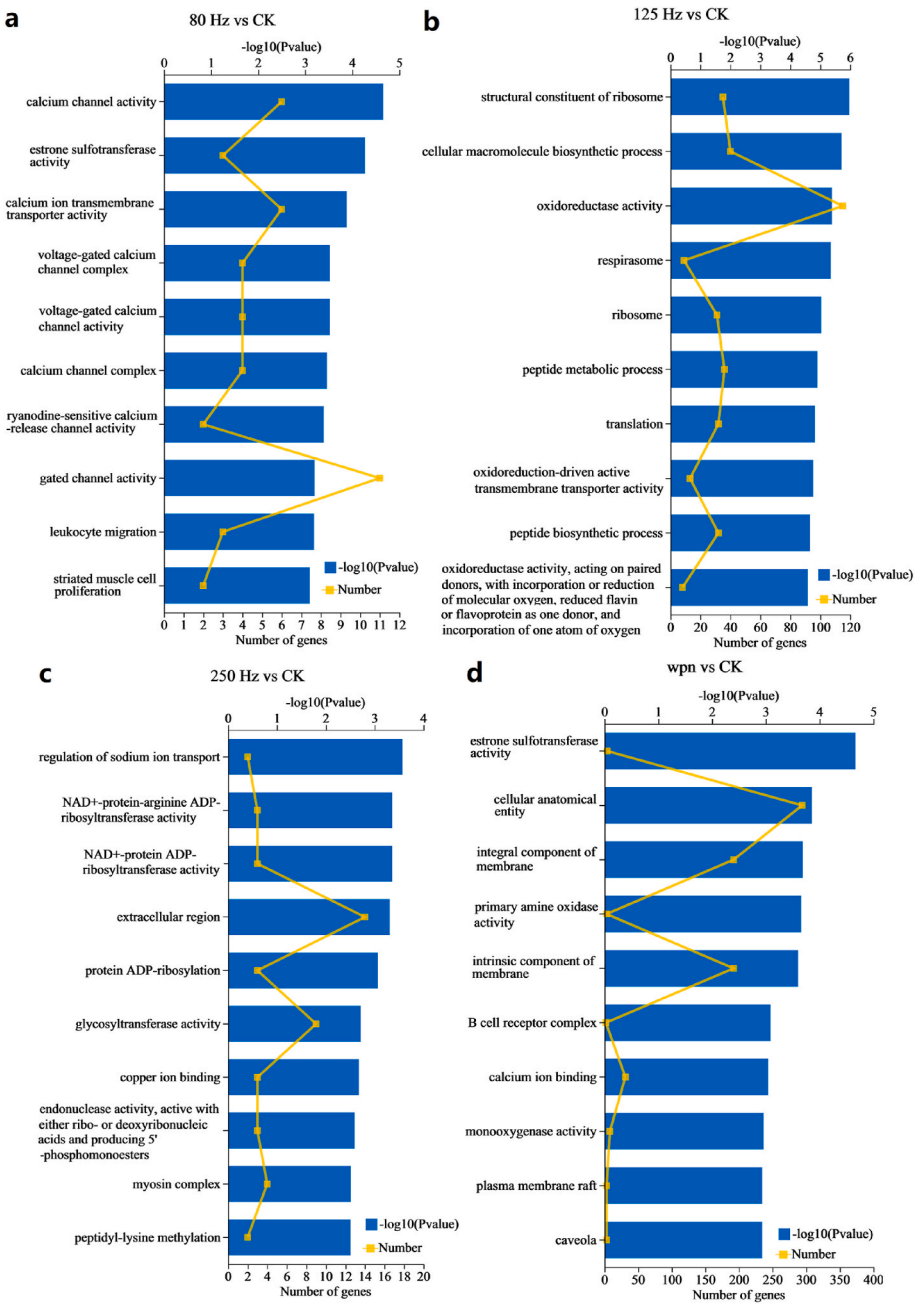

Fig. 8. The top 10 most significantly enriched GO terms from the differentially expressed genes of kidney, with a *P*-value of <0.05. a: CK vs 80 Hz group. b: CK vs 125 Hz group. c: CK vs 250 Hz group. d: CK vs wpn group.

3.2. GO annotations analysis of DEGs

DEGs can be classified into three major biological functions through Gene Ontology (GO) annotation: biological process, cellular component and molecular function, along with the subcategories within three major ontology. Fig. 5 displays the top 20 subcategories in terms of abundance. Across three tissues of the 80 Hz, 125 Hz, 250 Hz, and wpn groups in the biological process ontology, cellular process, biological regulation were the most prevalent terms. In the cellular component ontology, membrane part, cell part had the highest annotation proportions. In the molecular function ontology, binding, catalytic activity were the most abundant terms. In liver and kidney tissues, in addition to cellular process and biological regulation, the subcategory metabolic process also exhibits a substantial annotation proportion in the biological process ontology.

3.3. GO enrichment analysis of DEGs

To gain a comprehensive understanding of the biological functions associated with DEGs, GO enrichment analysis was conducted. For brain tissues (Fig. 6), in the 80 Hz group compared with the CK group, the three major functional categories that showed the most significant enrichment for DEGs were heme binding, tetrapyrrole binding, and sequence-specific DNA binding; In the 125 Hz group compared with the CK group, the three major functional categories that showed the most significant enrichment for DEGs were G protein-coupled amine receptor activity, digestion, and phosphoric diester hydrolase activity; In the 250 Hz group compared with the CK group, the three major functional categories that showed the most significant enrichment for DEGs were plasma membrane protein complex, molecular transducer activity, and signaling receptor activity; In the wpn group compared with the CK

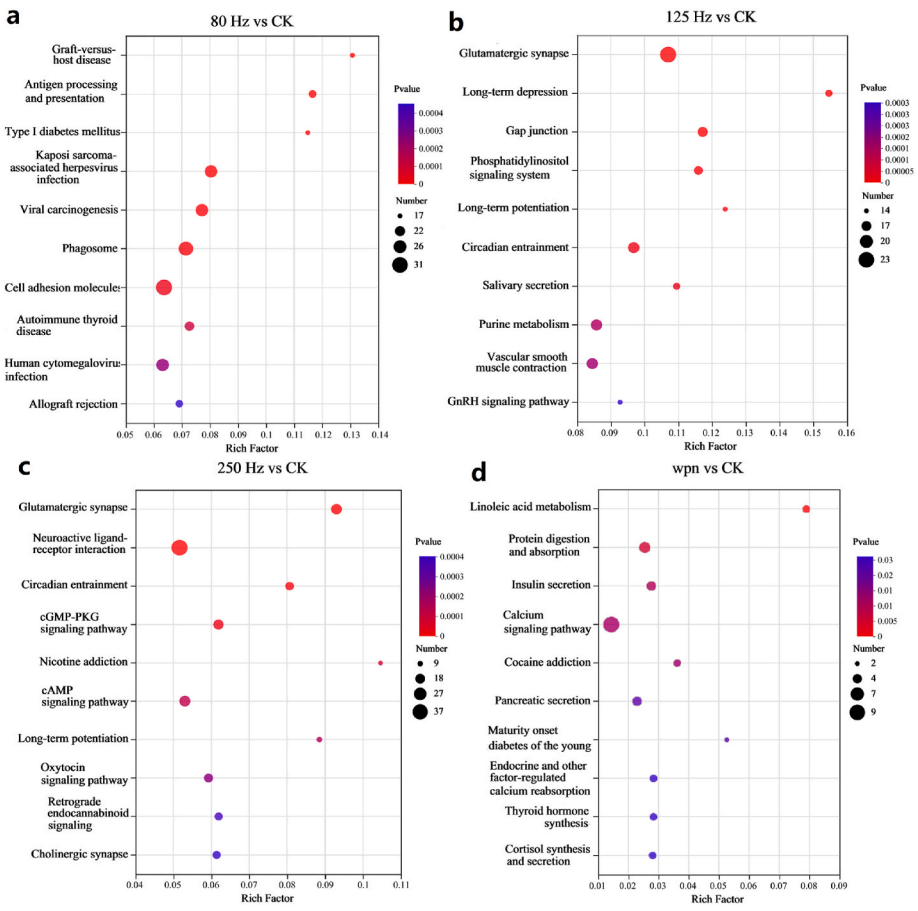

Fig. 9. The KEGG pathways enriched in DEGs of brain between the CK group and noise exposure groups, with a *P*-value of <0.05. a: CK vs 80 Hz group. b: CK vs 125 Hz group. c: CK vs 250 Hz group. d: CK vs wpn group.

group, the three major functional categories that showed the most significant enrichment for DEGs were heme binding, tetrapyrrole binding, and oxygen carrier activity.

For liver tissues (Fig. 7), in the 80 Hz group compared with the CK group, the three major functional categories that showed the most significant enrichment for DEGs were regulation of cell cycle, regulation of cell cycle process, and ribosomal small subunit export from nucleus; In the 125 Hz group compared with the CK group, the three major functional categories that showed the most significant enrichment for DEGs were thioester metabolic process, acetyl-CoA metabolic process, and ATP transmembrane transporter activity; In the 250 Hz group compared with the CK group, the three major functional categories that showed the most significant enrichment for DEGs were chitin binding, glycolytic process, and ATP generation from ADP; In the wpn group compared with the CK group, the three major functional categories that showed the most significant enrichment for DEGs were lipid biosynthetic process, organic hydroxy compound biosynthetic process, and sterol biosynthetic process.

For kidney tissues (Fig. 8), in the 80 Hz group compared with the CK group, the three major functional categories that showed the most significant enrichment for DEGs were calcium channel activity, estrone sulfotransferase activity, and calcium ion transmembrane transporter activity; In the 125 Hz group compared with the CK group, the three major functional categories that showed the most significant enrichment for DEGs were structural constituent of ribosome, cellular macromolecule biosynthetic process, and oxidoreductase activity; In the 250 Hz group compared with the CK group, the three major functional categories that showed the most significant enrichment for DEGs were regulation of sodium ion transport, NAD + -protein-arginine ADP-ribosyltransferase activity, and NAD + -protein ADP-ribosyltransferase activity; In the wpn group compared with the CK group, the three major functional categories that showed the most significant enrichment for DEGs were estrone sulfotransferase activity, cellular anatomical entity, and integral component of membrane.

3.4. KEGG pathway enrichment analysis of DEGs

Figs. 9–11 present the top 10 significantly enriched pathways obtained through KEGG pathway enrichment analysis of DEGs in the brain, liver, and kidney tissues of the experimental groups compared with the CK group. In the brain tissues, the most significantly enriched pathways were as follows. For the 80 Hz group: Graft-versus-host disease (GVHD), Antigen processing and presentation, and Type 1 diabetes mellitus (T1DM). For the 125 Hz group: Glutamatergic synapse, Long-term depression (LTD), and Gap junction. For the 250 Hz group: Glutamatergic synapse and Neuroactive ligand-receptor interaction. For the wpn group: Linoleic acid metabolism, Protein digestion and absorption.

In the liver tissues, the most significantly enriched pathways were as follows: For the 80 Hz group: Protein processing in endoplasmic reticulum, p53 signaling pathway and Cell cycle. For the 125 Hz group: PPAR signaling pathway and Steroid biosynthesis. For the 250 Hz group: Primary bile acid biosynthesis, Cholesterol metabolism and Vitamin digestion and absorption. For the wpn group: Steroid biosynthesis and Pancreatic secretion.

In the kidney tissues, the most significantly enriched pathways were as follows: For the 80 Hz group: Hypertrophic cardiomyopathy (HCM), Dilated cardiomyopathy (DCM), and Cardiac muscle contraction. For the 125 Hz group: Coronavirus disease, Hematopoietic cell lineage, and

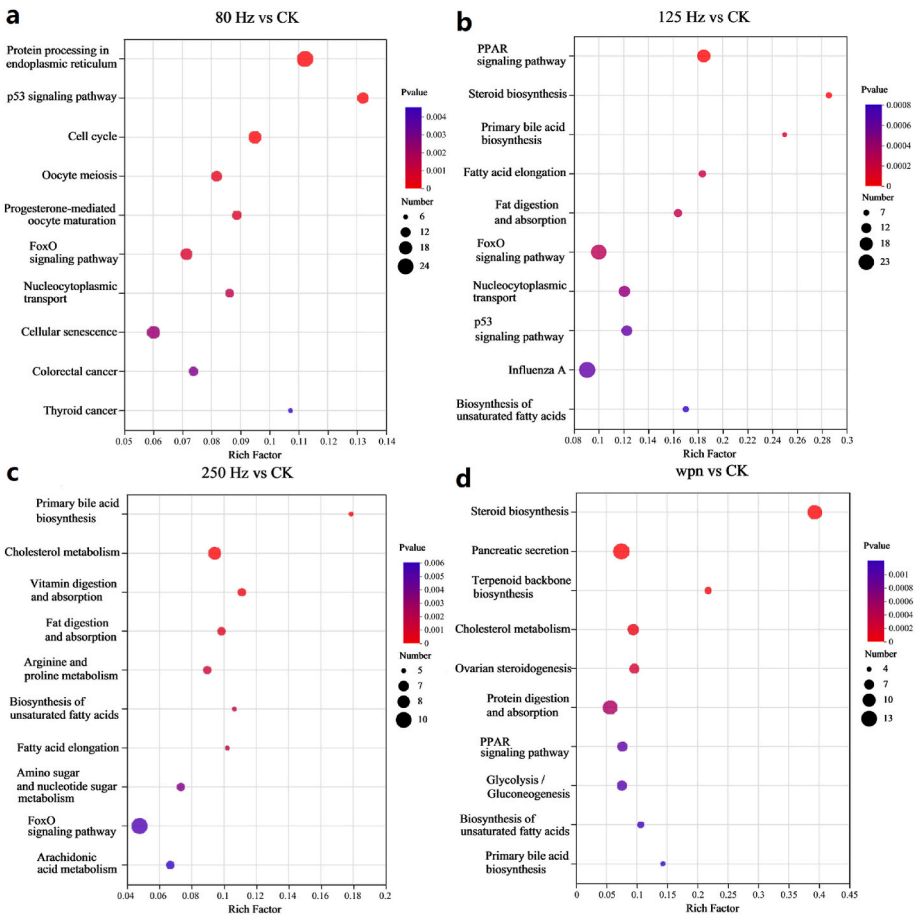

Fig. 10. The KEGG pathways enriched in DEGs of liver between the CK group and noise exposure groups, with a *P*-value of <0.05.
a: CK vs 80 Hz group. b: CK vs 125 Hz group. c: CK vs 250 Hz group. d: CK vs wpn group.

PI3K-Akt signaling pathway. For the 250 Hz group: Viral myocarditis (VMC), Dilated cardiomyopathy, Allograft rejection, and Autoimmune thyroid disease (AITD). For the wpn group: Insulin secretion and Graft-versus-host disease.

3.5. Validation of the RNA-seq results using RT-PCR methods

Real-time reverse transcription polymerase chain reaction (RT-PCR) was employed to validate the expression profiles of eighteen genes (six genes were selected for each tissue) identified through RNA-seq analysis. Notable alterations in gene expression were observed through both methodologies, including upregulation of *TUBA*, *SMOX*, *HSPA_5*, *TRAM1*, *MESO1*, *FDFT1*, *BPI*, *PRDX6*, *IGH*, *HSPA1s* as well as down-regulation of *SLC17A6_7_8*, *ERK*, *FABP4*, *CCK*, *FABP2*, *APOA4*, *FABP6*, *MHC1*. Consistency between the qRT-PCR results and RNA-seq data (Fig. 12) underscores the robustness of the RNA-seq findings.

4. Discussion

The current research on the genetic-level impacts of noise stress on fish is still in its early stages, particularly regarding the effects of long-term operational noise from offshore wind farms on gene expression and fish health in their vicinity, which necessitates further comprehensive investigation. This study unveiled significant differences in gene expression between the experimental groups (80 Hz, 125 Hz, 250 Hz, wpn) and the control group. Specifically, there were 1736, 4341, 1208, and 1333 genes exhibiting significant variations in expression respectively among juvenile *S. schlegelii*. The majority of DEGs were associated with GO enrichment and KEGG pathways related to metabolism, immune response, neural signal transmission, and disease. These findings indicate that the predominant frequencies of noise at 80 Hz, 125 Hz, and 250 Hz generated by long-term operation of existing offshore wind turbines as well as on-site noise have detrimental effects on the health of *S. schlegelii*.

4.1. Analysis of DEGs affecting auditory sensation

The inner ear, situated within the osseous structures bilaterally on either side of the cranium, functions as one of the auditory organs in teleost fish. Typically encompassing the utricle, saccule, and three semicircular canals, it also harbors otoliths exhibiting diverse shapes and sizes. When fish are exposed to sound-induced water particle movements, the otoliths experience diverse magnitudes and orientations of motion. This stimulation induces the deflection of cilia on the surface of sensory cells, leading to the release of neurotransmitters and subsequent transmission of signals to the brain via afferent neurons (Popper and Hawkins, 2019). The expression of two genes (*DCDC2* and *USH1C*) associated with auditory perception was found to be significantly regulated in the brain tissues of 80 Hz vs CK group and 125 Hz vs CK group in this study. The expression of gene *CLIC5* was found to be significantly upregulated in the kidney tissues of 125 Hz vs CK group. Grati et al. (2015) demonstrated that targeted disruption of the *DCDC2* homolog, *DCDC2B*, in zebrafish (*Danio rerio*) using *DCDC2B* morpholino-mediated knockdown resulted in profound degeneration of hair cells within the inner ear and lateral line neuromasts. This indicates the crucial role of the *DCDC2B* gene in the development and survival of sensory hair cells in zebrafish. The precise assembly of Usher syndrome (USH) proteins into intricately organized macromolecular complexes is

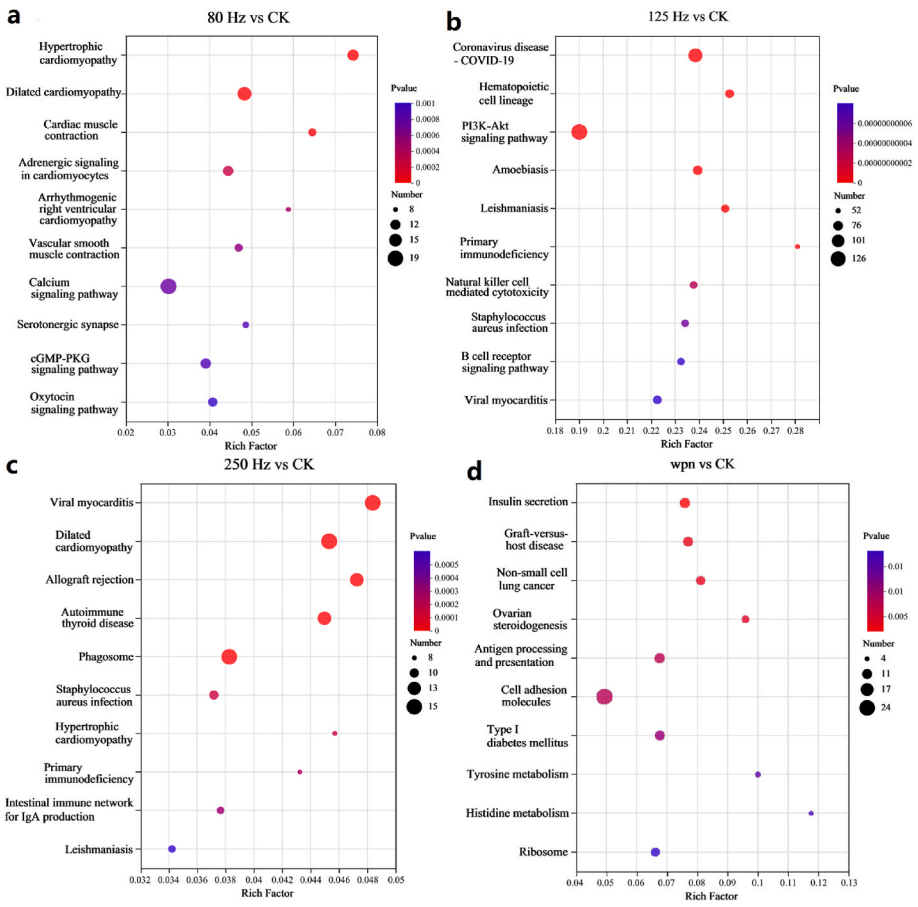

Fig. 11. The KEGG pathways enriched in DEGs of kidney between the CK group and noise exposure groups, with a *P*-value of <0.05. a: CK vs 80 Hz group. b: CK vs 125 Hz group. c: CK vs 250 Hz group. d: CK vs wpn group.

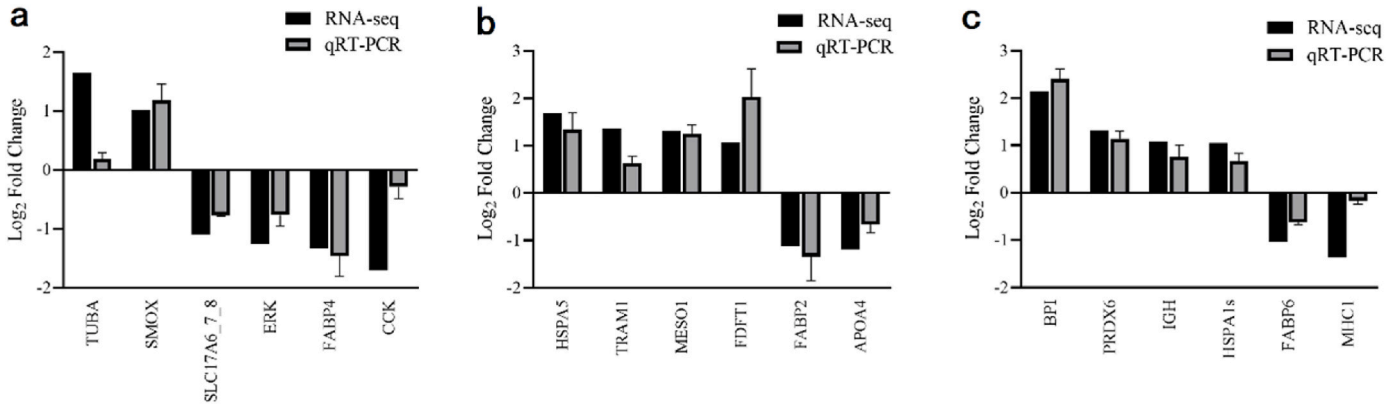

Fig. 12. Results of quantitative real-time polymerase chain reaction (qRT-PCR) and RNA sequencing (RNA-seq) for the selected differentially expressed genes in brain (a), liver (b), and kidney (c) tissues of *S. schlegelii*.

indispensable for the structural alterations in mechanoreceptors of hair cells within the inner ear, as well as for facilitating mechanoelectrical transduction (MET). Dysfunction of the pathogenic gene *USH1C* leads to structural and functional impairments in hair cells during development (Phillips et al., 2011). Chloride intracellular channel 5 (*CLIC5*) is deafness-linked proteins required for hearing in both humans and mice. It is necessary for proper development and maintenance of delicate sensory stereocilia of inner-ear hair cells (Waddell and Benjiamin, 2016). Additionally, our study unveiled significant enrichment in three auditory-related signaling pathways in the 125 Hz vs CK group and 250 Hz vs CK group: the glutamatergic synapse pathway (map 04724), the GABAergic synapse pathway (map 04727), and the cAMP signaling pathway (map 04024). Both glutamatergic and GABAergic synapses play pivotal roles in the auditory system (Joshi and Wang, 2002), while the cAMP signaling pathway is indispensable for the proliferation of sensory receptor epithelial cells in audition (Navaratnam et al., 1996). Based on the aforementioned findings, compared with the effects of measured noise, the dominant frequency noise generated by offshore wind farms, especially 80 Hz and 125 Hz, acting as a non-biological stressor, have the potential to disrupt the normal morphology of sensory hair cells in *S. schlegelii* and consequently impede its auditory functionality.

4.2. Analysis of DEGs affecting metabolism

In this study, a majority of GO functional enrichments were significantly associated with energy metabolism-related functions. For example, in the brain tissues of the 80 Hz and wpn groups, enrichments were observed in heme binding and tetrapyrrole binding. In the liver tissues of the 125 Hz group, enrichment was detected in the thioester metabolic process, while in the 250 Hz group, enrichment was noted in the glycolytic process. The study conducted by Sørensen et al. (2013) has demonstrated that prolonged exposure to noise stimuli can lead to alterations in metabolic regulation in mice, thereby increasing the susceptibility to developing metabolic syndrome. Lipids play a pivotal role in maintaining energy homeostasis and facilitating intracellular signal transduction. In this study, we observed the activation of pathways associated with cholesterol metabolism, arachidonic acid metabolism, steroid biosynthesis, and the PPAR signaling pathway in liver tissues of *S. schlegelii*. These findings suggest a potential impact of noise on lipid metabolism in *S. schlegelii*. Zhang Y et al. (2022) discovered that exposure to noise stress at a level of 120 dB resulted in the upregulation of genes associated with lipid metabolism in the sound-producing muscles of *Larimichthys polyactis*, thereby disrupting lipid metabolism. Pancreatic secretion is an integral component of digestive metabolism, specifically involving the excretion of digestive enzymes, which plays a pivotal regulatory role in facilitating food digestion and absorption (Hasegawa et al., 1993). The wpn group of *S. schlegelii* exhibited upregulation of genes associated with pancreatic secretion. Insulin, a product derived from pancreatic secretion, plays a crucial role in regulating blood glucose levels. The wpn group of *S. schlegelii* exhibited upregulation of genes associated with pancreatic secretion. Insulin, a product derived from pancreatic secretion, plays a crucial role in regulating blood glucose levels. The study revealed that the transcriptome exhibited a significant enrichment of pathways associated with *S. schlegelii* metabolism, suggesting that prolonged exposure to noise generated by offshore wind farms may potentially lead to metabolic disorders.

4.3. Analysis of DEGs related to immune response

The immune response plays a pivotal role in safeguarding organisms against diseases. Active regulation of the immune system enables the elimination of invading pathogens, thereby protecting the host, while an aberrant immune response can inflict harm upon the organism (Martin et al., 2019). The experimental groups of *S. schlegelii* exhibited significant enrichment in pathways associated with graft-versus-host disease (GVHD), antigen processing and presentation, allograft rejection, phagosomes, and autoimmune thyroid diseases. Antigen processing and presentation play pivotal roles in modulating immune responses (Santambrogio et al., 2019), while phagosomes serve as crucial sites for immune cells to degrade internalized pathogens (Yu et al., 2021). In the brain and liver tissues of *S. schlegelii*, we found fewer KEGG pathways directly related to immune regulation, with a predominant involvement of neural and metabolic functions. Conversely, in kidney tissues, particularly in the 250 Hz and wpn groups, we noted a significant enrichment of pathways associated with immune system modulation, highlighting distinct immunoregulatory effects across different frequency treatment groups. Furthermore, prolonged noise stress may also contribute to an increased incidence of myocardial diseases in *S. schlegelii*. The KEGG pathway analysis of kidney tissue in *S. schlegelii* revealed that the dominant frequency noise generated by wind turbines could potentially impact pathways associated with dilated cardiomyopathy, myocardial contraction, and viral myocarditis. These findings suggest that prolonged exposure to noise may have implications for the immune and cardiac health of *S. schlegelii*.

5. Conclusions

In summary, this study conducted a comprehensive analysis of gene expression in the brain, liver, and kidney tissues of *S. schlegelii* under the influence of dominant frequency and on-site noise stress induced by offshore wind turbines. The findings suggest that prolonged noise stress resulting from offshore wind farm operations induces alterations in gene expression in *S. schlegelii*, impacting neurotransmission pathways such as the glutamatergic synapse. Moreover, it suppresses lipid metabolism, leading to the upregulation of antigen processing and presentation genes, as well as endoplasmic reticulum protein processing genes, thereby triggering activation of the immune system in *S. schlegelii*. Noise stress can also impact pathways associated with dilated cardiomyopathy, myocardial contraction, and viral myocarditis, potentially leading to the development of myocardial diseases in *S. schlegelii*. In conclusion, the findings of this study demonstrate that both offshore wind turbines' underwater dominant frequency noise and on-site noise have varying degrees of impact on the metabolism and immune system of *S. schlegelii*. Therefore, it is recommended to implement effective measures aimed at reducing underwater noise during offshore wind turbine operation in order to ensure the overall health and well-being of fish in the surrounding marine environment.

CRediT authorship contribution statement

Yining Wang: Writing – original draft, Validation, Methodology, Investigation, Formal analysis, Data curation. **Kuangmin Gong:** Writing – original draft, Validation, Project administration, Funding acquisition, Formal analysis, Data curation. **Jun Xie:** Software, Project administration, Investigation. **Wei Wang:** Investigation, Data curation. **Jianhao Zheng:** Investigation, Formal analysis, Data curation. **Liuyi Huang:** Writing – review & editing, Supervision, Funding acquisition, Conceptualization.

Declaration of competing interest

The authors declare that they have no known competing financial interests or personal relationships that could have appeared to influence the work reported in this paper.

Data availability

Data will be made available on request.

Acknowledgement

This work was supported by the China Three Gorges Corporation [ZR2023MD090].

Appendix A. Supplementary data

Supplementary data to this article can be found online at https://doi.org/10.1016/j.marenvres.2024.106717.

References

Ali, S.W., et al., 2021. Offshore wind farm-grid integration: a review on infrastructure, challenges, and grid solutions. IEEE Access 9, 102811–102827. https://doi.org/10.1109/ACCESS.2021.3098705.

Andrews, C.D., et al., 2014. Identification of a gene set to evaluate the potential effects of loud sounds from seismic surveys on the ears of fishes: a study with Salmo salar. J. Fish. Biol. 84 (6), 1793–1819. https://doi.org/10.1111/jfb.12398.

Buscaino, G., Filiciotto, F., Buffa, G., Bellante, A., Di Stefano, V., Assenza, A., et al., 2010. Impact of an acoustic stimulus on the motility and blood parameters of European sea bass (Dicentrarchus labrax L.) and gilthead sea bream (Sparus aurata L.). Mar. Environ. Res. 69 (3), 136–142. https://doi.org/10.1016/j.marenvres.2009.09.004.

Butler, J.M., Maruska, K.P., 2021. Noise during mouthbrooding impairs maternal care behaviors and juvenile development and alters brain transcriptomes in the African cichlid fish Astatotilapia burtoni. Gene Brain Behav. 20 (3), e12692 https://doi.org/10.1111/gbb.12692.

Chandhini, et al., 2019. Transcriptomics in aquaculture: current status and applications. Rev. Aquacult. 11 (4), 1379–1397. https://doi.org/10.1111/raq.12298.

Chang, H.Y., Lin, T.H., Anraku, K., Shao, Y.T., 2018. The effects of continuous acoustic stress on ROS levels and antioxidant-related gene expression in the black porgy (Acanthopagrus schlegelii). Zool. Stud. 57 https://doi.org/10.6620/ZS.2018.57-59.
Chen, G.D., Decker, B., Muthaiah, V.P.K., Sheppard, A., Salvi, R., 2014. Prolonged noise exposure-induced auditory threshold shifts in rats. Hear. Res. 317, 1–8. https://doi.org/10.1016/j.heares.2014.08.004.
Chen, J., et al., 2022. Green development strategy of offshore wind farm in China guided by life cycle assessment. Resour. Conserv. Recycl. 188, 106652 https://doi.org/10.1016/j.resconrec.2022.106652.
Chen, S., et al., 2018. fastp: an ultra-fast all-in-one FASTQ preprocessor. Bioinformatics 34 (17), i884–i890. https://doi.org/10.1093/bioinformatics/bty560.
Chen, Y., Lin, H., 2022. Overview of the development of offshore wind power generation in China. Sustain. Energy Technol. Assessments 53, 102766. https://doi.org/10.1016/j.seta.2022.102766.
Cheng, X., et al., 2024. Transcriptomic analysis reveals the immune response mechanisms of sea cucumber Apostichopus japonicus under noise stress from offshore wind turbine. Sci. Total Environ. 906, 167802 https://doi.org/10.1016/j.scitotenv.2023.167802.
Cresci, A., et al., 2023. Atlantic cod (Gadus morhua) larvae are attracted by low-frequency noise simulating that of operating offshore wind farms. Commun. Biol. 6 (1), 353. https://doi.org/10.1038/s42003-023-04728-y.
Du-Ok, S., 2000. The hearing ability of black rockfish Sebastes inermis to underwater audible sound-1. The auditory threshold. Korean Journal of Fisheries and Aquatic Sciences 33 (6), 581–584 (no DOI).
Grati, M.H., et al., 2015. A missense mutation in DCDC2 causes human recessive deafness DFNB66, likely by interfering with sensory hair cell and supporting cell cilia length regulation. Hum. Mol. Genet. 24 (9), 2482–2491. https://doi.org/10.1093/hmg/ddv009.
Hall, J.R., et al., 2023. Snow crab (Chionoecetes opilio) hemocytes and hepatopancreas transcriptomes: identification, validation, and application of immune-relevant biomarkers of exposure to noise. Front. Mar. Sci. 10 https://doi.org/10.3389/fmars.2023.1198036.
Hasegawa, H., et al., 1993. Effect of islet hormones on secretin-stimulated exocrine secretion in isolated perfused rat pancreas. Dig. Dis. Sci. 38, 1278–1283. https://doi.org/10.1007/BF01296079.
Higgins, P., Foley, A., 2014. The evolution of offshore wind power in the United Kingdom. Renew. Sustain. Energy Rev. 37, 599–612. https://doi.org/10.1016/j.rser.2014.05.058.
Jensen, F., 1982. Numerical models of sound propagation in real oceans. OCEANS 82. IEEE. https://doi.org/10.1109/OCEANS.1982.1151749.
Joshi, I., Wang, L.Y., 2002. Developmental profiles of glutamate receptors and synaptic transmission at a single synapse in the mouse auditory brainstem. J. Physiol. 540 (3), 861–873. https://doi.org/10.1113/jphysiol.2001.013506.
Kendall, A.W., 1991. Developments in environmental biology of fishes. In: Noakes, David L.G. (Ed.), Rockfishes of the Genus Sebastes: Their Reproduction and Early Life History. Springer Verlag, Berlin, pp. 173–190.
Kenneth, J., Thomas, D. Schmittgen, 2001. Analysis of relative gene expression data using real-time quantitative PCR and the $2^{-\Delta\Delta CT}$ method. Methods 25 (4), 402–408. https://doi.org/10.1006/meth.2001.1262.
Kim, D., et al., 2015. HISAT: a fast spliced aligner with low memory requirements. Nat. Methods 12 (4), 357–360. https://doi.org/10.1038/nmeth.3317.
Kulkarni, S.S., Edwards, D.J., 2022. A bibliometric review on the implications of renewable offshore marine energy development on marine species. Aquaculture and Fisheries 7 (2), 211–222. https://doi.org/10.1016/j.aaf.2021.10.005.
Li, A., 2022. Centralization or decentralization: divergent paths of governing offshore wind between China and Japan. Energy Res. Social Sci. 84, 102426 https://doi.org/10.1016/j.erss.2021.102426.
Li, B., Dewey, C.N., 2011. RSEM: accurate transcript quantification from RNA-Seq data with or without a reference genome. BMC Bioinf. 12, 1–16. https://doi.org/10.1186/1471-2105-12-323.
Love, M.I., et al., 2014. Moderated estimation of fold change and dispersion for RNA-seq data with DESeq2. Genome Biol. 15 (12), 1–21. https://doi.org/10.1186/s13059-014-0550-8.
Love, M.S., et al., 2022. The Rockfishes of the Northeast Pacific. University of California Press, California.
Mai, Y., 2018. The Morphological Differences of Sonic Muscle between Male and Female and Noise-Stress Induced Gene Expression in Brain and Liver in the Marbled Rockfish, Sebastiscus Marmoratus, after Exposure to Noise. D. Phil.Thesis. Shanghai Ocean University.
Mann, D.A., Cott, P.A., Hanna, B.W., Popper, A.N., 2007. Hearing in eight species of northern Canadian freshwater fishes. J. Fish. Biol. 70 (1), 109–120. https://doi.org/10.1111/j.1095-8649.2006.01279.x.
Martin-Mateos, R., et al., 2019. Dysfunctional immune response in acute-on-chronic liver failure: it takes two to tango. Front. Immunol. 10, 973. https://doi.org/10.3389/fimmu.2019.00973.
Matthews, K.R., 1990. A telemetric study of the home ranges and homing routes of copper and quillback rockfishes on shallow rocky reefs. Can. J. Zool. 68 (11), 2243–2250. https://doi.org/10.1139/z90-312.
Navaratnam, D.S., et al., 1996. Proliferation in the auditory receptor epithelium mediated by a cyclic AMP–dependent signaling pathway. Nat. Med. 2 (10), 1136–1139. https://doi.org/10.1038/nm1096-1136.
Pertea, M., et al., 2015. StringTie enables improved reconstruction of a transcriptome from RNA-seq reads. Nat. Biotechnol. 33 (3), 290–295. https://doi.org/10.1038/nbt.3122.
Phillips, J.B., et al., 2011. Harmonin (Ush1c) is required in zebrafish Müller glial cells for photoreceptor synaptic development and function. Disease Models & Mechanisms 4 (6), 786–800. https://doi.org/10.1242/dmm.006429.
Popper, A.N., Hastings, M.C., 2009. The effects of anthropogenic sources of sound on fishes. J. Fish. Biol. 75 (3), 455–489. https://doi.org/10.1111/j.1095-8649.2009.02319.x.
Popper, A.N., Hawkins, A.D., 2019. An overview of fish bioacoustics and the impacts of anthropogenic sounds on fishes. J. Fish. Biol. 94 (5), 692–713. https://doi.org/10.1111/jfb.13948.
Popper, Arthur, N., et al., 2022. Offshore wind energy development: research priorities for sound and vibration effects on fishes and aquatic invertebrates. J. Acoust. Soc. Am. 151 (1), 205–215. https://doi.org/10.1121/10.0009237.
Santambrogio, L., et al., 2019. The antigen processing and presentation machinery in lymphatic endothelial cells. Front. Immunol. 10, 1033. https://doi.org/10.3389/fimmu.2019.01033.
Schuck, J.B., et al., 2011. Transcriptomic analysis of the zebrafish inner ear points to growth hormone mediated regeneration following acoustic trauma. BMC Neurosci. 12 (1), 1–20. https://doi.org/10.1186/1471-2202-12-88.
Sierra-Flores, et al., 2015. Stress response to anthropogenic noise in Atlantic cod Gadus morhua L. Aquacult. Eng. 67, 67–76. https://doi.org/10.1016/j.aquaeng.2015.06.003.
Smith, Michael E., Arthur, N. Popper, 2023. Temporary threshold shift as a measure of anthropogenic sound effect on fishes. In: The Effects of Noise on Aquatic Life: Principles and Practical Considerations. Springer International Publishing, Cham, pp. 1–14.
Smith, Michael E., et al., 2004. Noise-induced stress response and hearing loss in goldfish (Carassius auratus). J. Exp. Biol. 207 (3), 427–435. https://doi.org/10.1242/jeb.00755.
Soares-Ramos, E.P., et al., 2020. Current status and future trends of offshore wind power in Europe. Energy 202, 117787. https://doi.org/10.1016/j.energy.2020.117787.
Sørensen, M., et al., 2013. Long-term exposure to road traffic noise and incident diabetes: a cohort study. Environ. Health Perspect. 121 (2), 217–222. https://doi.org/10.1289/ehp.1205503.
Tu, Z., et al., 2021. Transcriptome analysis of the central nervous system of sea slug (Onchidium reevesii) exposed to low-frequency noise. Front. Mar. Sci. 8, 807489 https://doi.org/10.3389/fmars.2021.807489.
Waddell, B.B., 2016. CLIC5 Maintains Lifelong Structural Integrity of Sensory Stereocilia by Promoting Radixin Phosphorylation in Hair Cells of the Inner Ear (Bachelor's Thesis. Ohio University.
Wang, Y., et al., 2023. Experimental study on the effect of sound stimulation on hearing and behavior of juvenile black rockfish (Sebastes schlegelii). Front. Mar. Sci. 10, 3389. https://doi.org/10.3389/fmars.2023.1257473.
Winter, H.V., et al., 2010. Residence Time and Behaviour of Sole and Cod in the Offshore Wind Farm Egmond Aan Zee (OWEZ). No. OWEZ_R_265_T1_20100916. IMARES.
Yang, Y., et al., 2018. Transcriptome analysis reveals enrichment of genes associated with auditory system in swimbladder of channel catfish. Comp. Biochem. Physiol. Genom. Proteonomics 27, 30–39. https://doi.org/10.1016/j.cbd.2018.04.004.
Yu, Y., et al., 2021. Single-phagosome imaging reveals that homotypic fusion impairs phagosome degradative function. Biophys. J. 121 (3), 459–469. https://doi.org/10.1016/j.bpj.2021.12.032.
Zhang, X., et al., 2022. Transcriptomic and behavioral studies of small yellow croaker (Larimichthys polyactis) in response to noise exposure. Animals 12 (16), 2061. https://doi.org/10.3390/ani12162061.
Zhang, Y., et al., 2022. Multi-omics reveals response mechanism of liver metabolism of hybrid sturgeon under ship noise stress. Sci. Total Environ. 851, 158348 https://doi.org/10.1016/j.scitotenv.2022.158348.
Zhongshang Industrial Research Institute. Report on market prospects and development trends of China offshore wind power industry (2023-2028). Available at: https://www.askci.com/reports/20231008/152553847126967499544070 4086.shtml. (Accessed 3 November 2023).